*Proc. Natl. Acad. Sci. USA*
Vol. 92, pp. 11519–11523, December 1995
Biophysics

# Proton transport by a bacteriorhodopsin mutant, aspartic acid-85 → asparagine, initiated in the unprotonated Schiff base state

**(photovoltage/photocycle/purple membrane)**

S. DICKOPF*, U. ALEXIEV*, M. P. KREBS†‡, H. OTTO*, R. MOLLAAGHABABA†, H. G. KHORANA†, AND M. P. HEYN*

*Biophysics Group, Department of Physics, Freie Universität Berlin, Arnimallee 14, D-14195 Berlin, Germany; and †Departments of Biology and Chemistry, Massachusetts Institute of Technology, 77 Massachusetts Avenue, Cambridge, MA 02139

*Contributed by H. G. Khorana, August 29, 1995*

**ABSTRACT** **At alkaline pH the bacteriorhodopsin mutant D85N, with aspartic acid-85 replaced by asparagine, is in a yellow form ($\lambda_{max} \approx 405$ nm) with a deprotonated Schiff base. This state resembles the M intermediate of the wild-type photocycle. We used time-resolved methods to show that this yellow form of D85N, which has an initially unprotonated Schiff base and which lacks the proton acceptor Asp-85, transports protons in the same direction as wild type when excited by 400-nm flashes. Photoexcitation leads in several milliseconds to the formation of blue (630 nm) and purple (580 nm) intermediates with a protonated Schiff base, which decay in tens of seconds to the initial state (400 nm). Experiments with pH indicator dyes show that at pH 7, 8, and 9, proton uptake occurs in about 5–10 ms and precedes the slow release (seconds). Photovoltage measurements reveal that the direction of proton movement is from the cytoplasmic to the extracellular side with major components on the millisecond and second time scales. The slowest electrical component could be observed in the presence of azide, which accelerates the return of the blue intermediate to the initial yellow state. Transport thus occurs in two steps. In the first step (milliseconds), the Schiff base is protonated by proton uptake from the cytoplasmic side, thereby forming the blue state. From the pH dependence of the amplitudes of the electrical and photocycle signals, we conclude that this reaction proceeds in a similar way as in wild type—i.e., via the internal proton donor Asp-96. In the second step (seconds) the Schiff base deprotonates, releasing the proton to the extracellular side.**

Bacteriorhodopsin is a light-driven proton pump that transports protons from the cytoplasmic to the extracellular side of the purple membrane (for a review, see ref. 1). The retinal chromophore is bound to the opsin by a protonated Schiff base (SB) linkage and is located approximately halfway between the two sides of the membrane. After absorption and isomerization, the pK of the SB drops, the SB deprotonates, and a proton is transferred to Asp-85 in the transition between the L and M intermediates (10–100 $\mu$s). Concomitantly a proton is released on the extracellular side. Subsequently the deprotonated 13-cis chromophore in M is reprotonated from Asp-96, which is located near the cytoplasmic surface. Asp-96 is in turn reprotonated from the cytoplasmic surface in the millisecond transition between the N and O intermediates. The functional cycle thus consists of two half cycles: the first half for proton release from the protonated SB to the extracellular side via Asp-85 (microseconds) and the second half for reprotonation of the deprotonated SB from the cytoplasmic side via Asp-96 (milliseconds).

At neutral pH the mutant D85N, which lacks the acceptor Asp-85, is inactive as a proton pump and has a red-shifted chromophore (615 nm) due to the absence of the negative charge of the counterion Asp-85 (2, 3). The pK of the SB of D85N is reduced to between 8 and 9 (depending on the ionic strength), suggesting that Asp-85 plays a major role in the SB counterion (3–5). Above the pK, the SB deprotonates and a yellow (405 nm) M-like state with a deprotonated SB is formed in the dark (3). The pH-dependent equilibrium is in fact more complicated, with a purple N-like state (570 nm) between the blue O-like and yellow M-like states (6, 7). We recently showed by time-resolved photovoltage measurements that when this N-like form is excited at pH 10.8 by 580-nm flashes, net proton pumping occurs in the same direction as in wild type (8). Here we investigate the proton pumping capacity of the yellow M-like form of D85N when excited with blue (400 nm) flashes by time-resolved flash spectroscopy and by kinetic measurements of the photovoltage and of the proton release and uptake. The recent observation of a small steady-state proton current when oriented membranes of the mutant D85N were illuminated by continuous blue light at pH 6.7 suggested that net proton pumping is taking place (9). With an initially unprotonated SB we may predict that net proton transport could occur in the same direction as in wild type provided that proton uptake precedes proton release. The first part of this new cycle could thus be quite similar to the second half of the wild-type cycle—i.e., protonation of the SB via Asp-96 and uptake from the cytoplasmic side in milliseconds. The second part may be expected to be slowed down due to the absence of the acceptor Asp-85 (release). These expectations were borne out by our experimental results.

## MATERIALS AND METHODS

The bacteriorhodopsin mutant D85N, in which Asp-85 is replaced by Asn, was prepared as described (10).

Flash spectroscopy and data analysis with a global exponential fit were performed as described elsewhere (11). Excitation was with 15-ns flashes of 1–3.5 mJ of energy at 400 nm.

Proton release and uptake kinetics were measured with pH indicator dyes at pH 7.0, 8.0, and 9.0. The following dyes were used: pyranine and fluorescein at pH 7.0, phenol red at pH 8.0, and xylenol blue at pH 9.0. With pyranine the difference of the flash-induced absorbance change was measured at 450 nm between samples with and without the dye. For the other dyes, the flash-induced absorbance differences between samples with and without a buffer mixture containing 3 mM each of Hepes, Trizma base, sodium acetate, and sodium carbonate were measured. The measuring wavelengths were 490 nm (fluorescein), 560 nm (phenol red), and 600 nm (xylenol blue).

Photovoltage measurements were performed at 22°C as described (8, 12, 13) with the following modifications. By using

The publication costs of this article were defrayed in part by page charge payment. This article must therefore be hereby marked "*advertisement*" in accordance with 18 U.S.C. §1734 solely to indicate this fact.

Abbreviations: SB, Schiff base; D85N and D96N, bacteriorhodopsin mutants containing an aspartic acid to asparagine substitution at position 85 or 96, respectively.

‡Present address: Department of Biomolecular Chemistry, University of Wisconsin Medical School, Madison, WI 53706.

a 2-$\mu$m polyester film (Hostaphan RE; a kind gift of Hoechst Diafoil, Wiesbaden, Germany) and a very large shunt resistance of 30 G$\Omega$, the first system discharge time $\tau_2^{sys}$ was increased to 12 s. The second system discharge time $\tau_2^{sys}$ was $\approx$150 s. A homemade circuit using operational amplifiers [Burr Brown model 3554 (Tucson, AZ) and Analog Devices model 9610 (Norwood, MA)] amplified the voltage by a factor of 100. The system rise time was $\approx$50 ns. Excitation by 400-nm flashes was as described above. Digitization of the voltage was performed using a digital oscilloscope [Le Croy model 9350 M (Chestnut Ridge, NY)] and a PC board [IMTEC model T 512 (Backnang, Germany)]. These provide two independent time bases (typical sampling times of 2 ns and 50 $\mu$s, respectively), amplifiers (minimum full range of 16 mV and 125 mV), analog/digital converters (8- and 12-bit), and on-board memory (250 kilobytes and 4 megawords). The signal was recorded simultaneously in these two trigger-coupled channels. The data from the two channels were merged into one set, which was reduced to $\approx$920 data points on a logarithmic time scale. The data were analyzed with a sum of exponentials and Gauss-distributed kinetics (12).

## RESULTS

**Spectroscopic Titration.** The pH dependence of the absorption spectra of D85N was recorded between pH 6.5 and 11.5 in steps of 0.5 pH units (Fig. 1). An isosbestic point was observed at 460 nm. The transition is more complex, however, than a simple two-state equilibrium between a blue, low-pH state absorbing around 615 nm and a yellow, high-pH form absorbing around 405 nm. That at least one more species contributes is apparent from the clear blue shift of the high wavelength absorption maximum to 570 nm above pH 9. Analysis of the spectroscopic titration data over the whole wavelength range using standard procedures (14) leads to apparent pK values of 8.2 and 9.6 for the deprotonation of the SB (100 mM NaCl). The first pK is between the blue form and the yellow form; the second is between the blue and a combination of purple and yellow. The yellow M-like state has a deprotonated SB, whereas the purple and blue forms have a protonated SB.

**Photocycle Kinetics.** The kinetics of the photocycle of D85N after excitation by a 400-nm flash was measured in steps of 10 nm at 34 wavelengths from 370 to 700 nm at pH 8. Fig. 2 is a two-dimensional contour plot of the absorbance difference $\Delta A(\lambda, t)$ as a function of time and wavelength. The main features of the cycle are apparent: bleaching of the yellow form leads to the formation of a blue state around 600 nm on the millisecond time scale. This blue form, which has a protonated SB, decays again in tens of seconds into the yellow initial state. The spectral width of the positive absorbance change in the red is unusually broad, suggesting that it may consist of at least two intermediates. This is borne out by the amplitude spectra $\Delta A_i(\lambda)$ that result from a global fit of the $\Delta A(\lambda, t)$ data to a sum of five exponentials with time constants $\tau_i$. With data at every 10 nm, these amplitude spectra (Fig. 3) have a reasonable wavelength resolution. Fig. 3 shows that the first rise time $\tau_1$ (1.9 ms) leads to the formation of a species with an absorption maximum around 580 nm ("purple"), whereas the slower second rise time $\tau_2$ (11 ms) produces an intermediate that absorbs further into the red, around 630 nm ("blue"). Both wavelength maxima have considerable error ($\pm$15 nm). The spectrum $\Delta A_3(\lambda)$ with $\tau_3$ = 190 ms has only a very small amplitude and may involve a transition from the purple (580 nm) to blue (630 nm) intermediate. The purple and blue intermediates decay again (possibly together) into the yellow initial state with times of 5.4 s ($\tau_4$) and 63 s ($\tau_5$). The amplitude spectra all cross the wavelength axis between 460 and 470 nm, which is close to the isosbestic point observed in the pH titration (Fig. 1).

The pH dependence of the photocycle kinetics was measured at 410, 590, and 670 nm from pH 7 to 11 (data not shown). Between pH 7 and 10, the amplitudes of the intermediates and the depletion signal increase with pH. This is

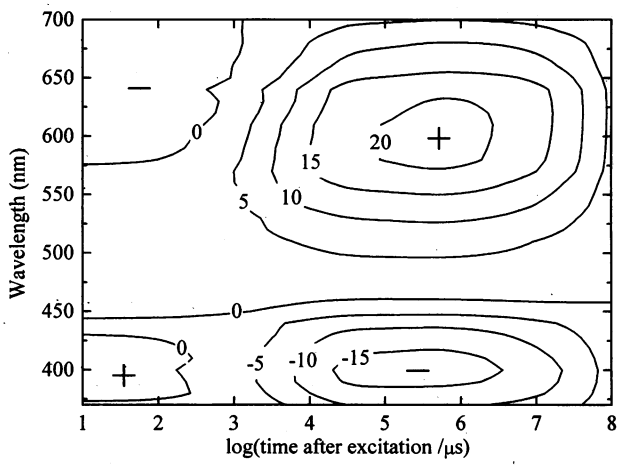


FIG. 2. Contour plot of the fit to the photocycle data $\Delta A(\lambda, t)$ for D85N. The photocycle was measured at 34 wavelengths from 370 to 700 nm. Conditions were pH 8, 150 mM $K_2SO_4$, 22°C, 3 mM standard buffer mixture, and excitation at 400 nm. The numbers labeling the contour lines of constant $\Delta A$ are the corresponding $\Delta A$ values multiplied by $10^3$.

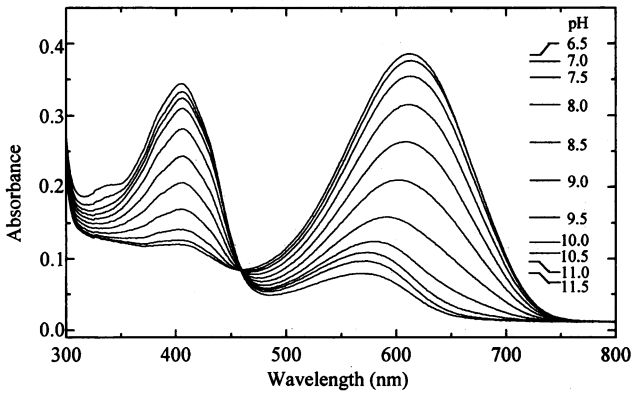


FIG. 1. pH dependence of the visible absorption spectra of the mutant D85N embedded in a polyacrylamide gel. The pH was increased in steps of 0.5 from 6.5 (top curve at 615 nm) to 11.5 (bottom curve) by adding NaOH. Conditions were 21°C, dark adapted, 100 mM NaCl, and 1 mM sodium phosphate.

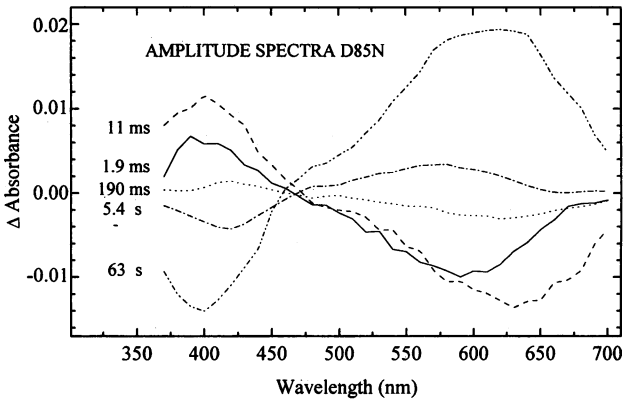


FIG. 3. Amplitude spectra $\Delta A_i(\lambda)$ corresponding to the five exponential time constants $\tau_i$ required in a global fit of the data of Fig. 2. A quasi-isosbestic point is apparent near 470 nm. The five time constants are listed. Experimental conditions were as in Fig. 2.

expected on the basis of the titration data, which indicate an increasing amount of the M-like initial state. Between pH 10 and 11 the photocycle amplitudes start to decrease again. This effect, which is also observed for the photovoltage signal, is most likely due to the deprotonation of Asp-96. If the protonated internal donor Asp-96 is required for the protonation of the SB, this reaction is expected to be blocked above the pK of Asp-96. Whereas at pH 8 the amplitude of the blue intermediate is largest (Fig. 3), at higher pH the purple form with the faster rise time predominates (data not shown). On the basis of the titration data, which indicate that between pH 7 and 9 the yellow form is mainly in equilibrium with a blue state, whereas between pH 9 and 11 the equilibrium is with a purple form, the photocycle results may be interpreted in terms of parallel cycles. The two parallel cycles, with blue and purple intermediates, respectively, have relative amplitudes that vary according to the pH-dependent equilibrium between the blue and purple forms in the initial state.

Fig. 4 *Inset* shows that at pH 8 the addition of azide strongly accelerates the decay of the blue form (measured at 650 nm) without affecting its rise. The mean decay times are 63.4, 25.4, 7.2, and 4.2 s in the presence of 0, 10, 50, and 100 mM azide, respectively.

**Kinetics of Proton Release and Uptake.** The kinetics of proton release and uptake were measured for D85N at pH 7 with pyranine and fluorescein, at pH 8 with phenol red, and at pH 9 with xylenol blue. At each pH, proton uptake preceded release. Fig. 5 shows the data at pH 8 and 32°C. In Fig. 5 *Lower*, the absorbance increase around 2.8 ms corresponds to the proton uptake, whereas the absorbance decrease around 6.3 s reflects the proton release. The proton kinetics correlates well with the time course of the blue intermediate (measured at 670 nm), with major rise and decay times of 2.7 ms and 9 s, respectively (Fig. 5 *Upper*). Similar results were obtained at the other pH values (data not shown). The uptake times [all values refer to 22°C, except for pH 8.0 (32°C)] are 6 ms (pyranine) and 9 ms (fluorescein) at pH 7.0; 3 ms at pH 8.0; and 10 ms at pH 9.0. The release times are 2 s (pyranine) and 3.6 s (fluorescein) at pH 7.0; 6.3 s at pH 8.0; and 9.4 s at pH 9.0. At pH 8.0 the stoichiometry of proton uptake and release was ≈1.

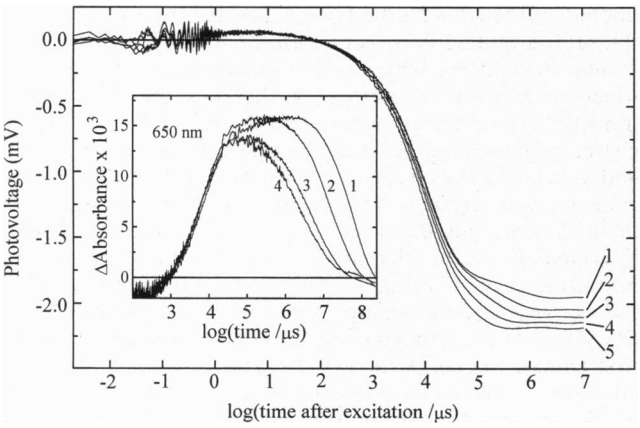


FIG. 4. Effect of azide on the photovoltage and photocycle of D85N excited in the yellow form with 400-nm flashes. (*Inset*) Rise and decay of the blue intermediate (650 nm) at pH 8, 150 mM $K_2SO_4$, and 3 mM standard buffer mixture. For curves 1–4 of the *Inset* the azide concentrations were 0, 10, 50, and 100 mM, and the mean decay times were 63.4, 25.4, 7.2, and 4.2 s, respectively. The five photovoltage traces labeled 1–5 correspond to azide concentrations of 0, 1, 2, 5, and 10 mM, respectively. The passive system discharge was subtracted as in ref. 12. Conditions for the electrical experiments were 22°C, pH 7.1, 150 mM $K_2SO_4$, and 3 mM each of Hepes, Trizma base, and sodium acetate. The nanosecond electrical component differs from that in Fig. 6 due to the contribution of the blue cycle at this lower pH.

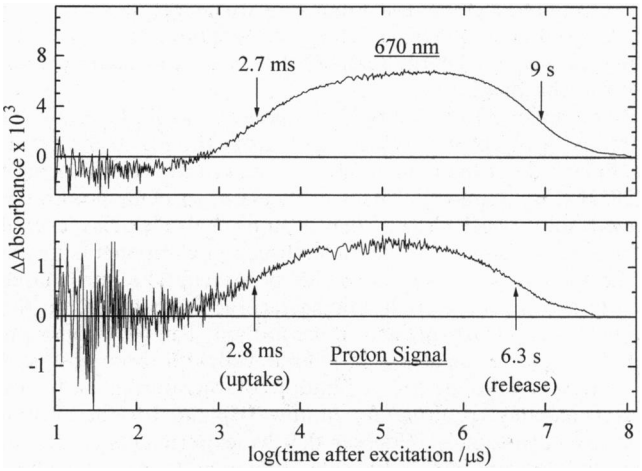


FIG. 5. Comparison of the kinetics of the rise and decay of the blue intermediate of D85N (*Upper*; protonated SB; monitored at 670 nm) with the kinetics of the proton release and uptake as detected by the dye phenol red (*Lower*; 560 nm). For both measurements conditions were pH 8.0, 32°C, and 150 mM $K_2SO_4$. Positive and negative absorbance changes for the dye indicate proton uptake and release, respectively. The rise and decay times indicated by the arrows were determined from exponential fits.

**Photovoltage Kinetics.** The time-resolved photovoltage signals of the yellow form of D85N and of wild type are compared in Fig. 6. In both cases, net charge motion was observed until the system discharged at ≈12 s ($\tau_1^{sys}$). Since the mutation does not affect the surface charge of the membrane, it is reasonable to assume that the orientation of the adsorbed membranes is the same for both samples. We can then conclude from Fig. 6 that protons are moved in the same direction when wild type is excited at 532 nm or when the yellow form of D85N is excited at 400 nm. In D85N, protons are thus transported in the direction from the cytoplasmic to the extracellular side of the membrane.

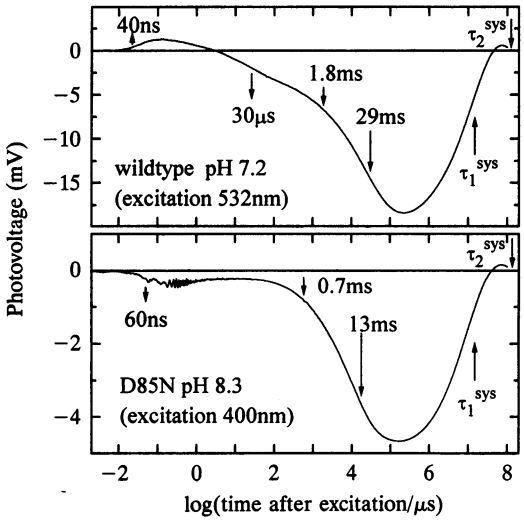


FIG. 6. Comparison of the time-resolved photovoltage signals from wild type (*Upper*; excited at 532 nm, pH 7.2) and the yellow form of D85N (*Lower*; excited at 400 nm, pH 8.3). Conditions were 22°C, 150 mM $K_2SO_4$, and 3 mM each of Hepes, Trizma base, and sodium acetate. Arrows indicate the time constants, sign, and relative amplitudes of the major active components in the charge movement. The passive discharge times of the system $\tau_1^{sys}$ and $\tau_2^{sys}$ have values of 12 and 150 s, respectively. With the membranes adsorbing with their extracellular side to the support, downward pointing arrows correspond to protons moving in the direction from the cytoplasmic to the extracellular side of the membrane.

Around 60 ns there is a minor forward charge movement for D85N. This component (not resolved with our time resolution) may be due to a charge redistribution after the isomerization of the chromophore.

The major 30-$\mu$s electrical component of wild type, associated with the proton release path from the SB to the extracellular side of the membrane, is absent in the yellow form of D85N (Fig. 6 *Lower*). This is in excellent agreement with the dye results, which showed that proton release is delayed until the second range. The major millisecond components of the wild-type signal, associated with proton uptake and charge motion from the cytoplasmic surface to the SB, are, on the other hand, clearly present in the mutant. The time constants (0.7 ms and 13 ms at pH 8.3) agree well with those observed for the kinetics of the formation of the purple and blue intermediates (protonation of the SB) and for the proton uptake (dye signal). Whereas the dye experiments could not provide information on the side of the membrane from which the proton is taken up, the electrical measurements show that the direction of charge motion is from the cytoplasmic to the extracellular side. A proton is thus taken up from the cytoplasmic side in several milliseconds.

The two millisecond electrical time constants (fast $\approx$ 1 ms; slow $\approx$ 10 ms) are roughly pH independent, but the corresponding amplitudes vary strongly with pH (Fig. 7). As for the photocycle amplitudes, the electrical signal increases above pH 7 since it is associated with the M-like yellow state, which is formed with a pK of 8.2. Above pH 10, the amplitude of the photovoltage decreases again, which is most likely due to the deprotonation of the internal donor Asp-96 (see *Discussion*). A fit of the sum of the two electrical amplitudes of Fig. 7 with the Henderson–Hasselbalch equation leads to apparent pK values of 7.4 and 10.5 for the increasing and decreasing part of the curve, respectively. These values are in good agreement with the first pK of the SB (8.2) and the pK of Asp-96 [11.4 (15)], if we recall that the pK values obtained from photovoltage measurements with adsorbed purple membranes are about one unit smaller than those obtained with purple membranes in suspension (3, 8, 13). The slow and fast electrical components predominate below and above pH 9.0, respectively (Fig. 7). According to the photocycle results, these two time constants are associated with the formation of the blue and purple intermediates, respectively. The observed acceleration of the photovoltage kinetics in the millisecond range with a pK of around 9.0 is thus probably a consequence of the spectroscopic titration (Fig. 1), which indicated that above (below) the pK of 9.6 the yellow form is mainly in equilibrium with the purple (blue) form.

Above pH 9.0, the photovoltage trace contains an additional very slow component in the forward direction with a time constant that increased from $\approx$100 ms at pH 10 to 1.1 s at pH 11.5. Such a slow pH-dependent component was also observed for wild type at alkaline pH and was attributed to the reprotonation of Asp-96 from the cytoplasmic surface (11).

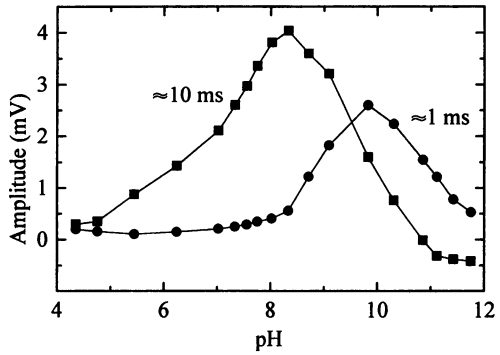


FIG. 7. pH dependence of the amplitude of the two components in the photovoltage of D85N with time constants of $\approx$1 ms and $\approx$10 ms (22°C).

The 400-nm flashes will also excite the photocycle of the blue form of D85N, which is the major species below the pK of 8.2, by absorption into a higher excited state. The time-resolved photovoltage of this low-pH blue form is well known (8). We estimate that its contribution to the photovoltage signal reported here is only 4.5% at pH 8.6 and negligible at higher pH.

With a first system discharge time $\tau_1^{sys}$ of 12 s, the charge displacement associated with the deprotonation of the SB and the proton release cannot be resolved electrically since they are slower. The decay of the blue intermediate at pH 8 is, however, accelerated from 63.4 s in the absence of azide to 4.2 s in 100 mM azide (Fig. 4 *Inset*). The photovoltage measurements were therefore performed at pH 7.1 in the presence of azide. At this lower pH, azide, which has a pK of 4.8, is more effective. Fig. 4 shows that with increasing azide concentration a further slow electrical component occurs, which has the same sign as the millisecond component and which is not completely resolved. This is clear evidence for proton movement in the direction from the cytoplasmic to the extracellular surface in seconds. For clarity the passive system discharge was substracted numerically using equation 2 of ref. 12.

## DISCUSSION

Analysis of the spectroscopic titration data revealed apparent pK values of 8.2 and 9.6, which characterize the equilibrium between the low-pH blue O-like state and the higher pH yellow M-like and purple N-like states. The deprotonation of the SB of D85N was first analyzed in this way by Turner *et al.* (6), who obtained pK values of 7.9, 9.2, and 11.5. According to their model, the M-like species is in rapid equilibrium with the purple N-like state, which is formed by reprotonation of the SB from Asp-96.

The photocycle measurements with the yellow form of D85N show that an intermediate with a protonated SB is formed in several milliseconds (blue or purple), which returns to the yellow initial state (deprotonated SB) in tens of seconds. The dye experiments indicate that the millisecond proton uptake correlates with the rise of the blue intermediate, and the proton release correlates with its decay. Neither experiment provides information on the side of the membrane from which protons are taken up or on the question of net proton transport. The electrical measurements define the direction of charge motion. Together with the results from the photocycle and dye measurements, the electrical data provide unequivocal evidence that a proton is taken up from the cytoplasmic side on the millisecond time scale. The very slow decay of the blue intermediate was accelerated to 4.2 s in the presence of 100 mM azide at pH 8.0 (Fig. 4). This allowed the observation of the charge motion associated with the slow deprotonation of the SB, since the corresponding time was now faster than the first passive discharge time of the electrical apparatus. The addition of azide had no effect on the millisecond components of the photocycle and photovoltage (Fig. 4) but led to the appearance of an additional electrical component in the direction from the cytoplasmic to the extracellular side of the membrane on the second time scale. Our experiments suggest that in this mutant azide acts as a proton acceptor on the extracellular side of the membrane. Since the decay time of the blue form is only slightly faster than the first discharge time in the presence of azide, the amplitude and time of this forward electrical component still cannot be determined quantitatively, but its sign and order of magnitude are certain. We thus conclude that net proton transport occurs with release to the extracellular side.

Under continuous blue light illumination, a small steady-state photocurrent was recently observed for the yellow form of D85N at pH 6.7, which increased 50-fold in the presence of 50 mM azide (9). Since the measurements were performed under light-saturating conditions, this effect is explained by our observation that azide accelerates the rate-limiting step of the cycle (Fig. 4). The steady-state current, which was shown to be due to protons (9), was in the same direction as observed in our experiments and is in excellent agreement with the kinetic data presented here.

As in wild type, the protonation of the SB and proton uptake occur in the millisecond time range from the cytoplasmic side of the membrane. With the mutation located between the chromophore and the extracellular side of the membrane, it is reasonable to assume that the proton uptake pathway from the cytoplasmic surface requires, as in wild type, the internal proton donor Asp-96. The pK of Asp-96 was recently shown to be ≈11.4 (15). If the protonated donor Asp-96 is necessary for the millisecond reprotonation of the SB, the associated charge movement is expected to decrease starting about 1 pH unit below its pK. The observed decrease of the electrical (Fig. 7) and photocycle signals above pH 10.5 thus strongly supports this model. Further evidence for the participation of Asp-96 in the protonation of the SB comes from Fourier-transform IR measurements, which detected a deprotonated Asp-96 in the blue intermediate of the D85N cycle (16). Moreover, those authors observed that in the yellow form of the double mutant D85N/D96N the rise of the blue intermediate (proton uptake) was slowed down 4000-fold compared to the single mutant D85N. However, in contrast to our results, Kataoka *et al.* (16) concluded that at pH 8.9 and 3 M KCl the proton is released on the cytoplasmic side—i.e., that no net transport occurs. This discrepancy may be due to the different experimental conditions.

We conclude that the yellow form of D85N with a deprotonated SB is active as a proton pump, with a reversal of the normal sequence of proton release and uptake. In the absence of the acceptor Asp-85, the cycle is slower but the direction of pumping is the same as in wild type.

We thank Dr. Stephan Moltke for a critical reading of the manuscript. This research was supported by Grant GM28289 from the National Institutes of Health (H.G.K.) and by Grant Sfb 312/B1 from the Deutsche Forschungsgemeinschaft (M.P.H.).

1. Mathies, R. A., Lin, S. W., Ames, J. B. & Pollard, W. T. (1991) *Annu. Rev. Biophys. Chem.* **20,** 491–518.
2. Mogi, T., Stern, L. J., Marti, T., Chao, B. H. & Khorana, H. G. (1988) *Proc. Natl. Acad. Sci. USA* **85,** 4148–4152.
3. Otto, H., Marti, T., Holz, M., Mogi, T., Stern, L. J., Engel, F., Khorana, H. G. & Heyn, M. P. (1990) *Proc. Natl. Acad. Sci. USA* **87,** 1018–1022.
4. Marti, T., Rösselet, S. J., Otto, H., Heyn, M. P. & Khorana, H. G. (1991) *J. Biol. Chem.* **266,** 18674–18683.
5. Marti, T., Otto, H., Rösselet, S. J., Heyn, M. P. & Khorana, H. G. (1992) *J. Biol. Chem.* **267,** 16922–16927.
6. Turner, G., Miercke, L. J. W., Thorgeirson, T. E., Kliger, D. S., Betlach, M. C. & Stroud, R. M. (1993) *Biochemistry* **32,** 1332–1337.
7. Brown, L. S., Bonet, L., Needleman, R. & Lanyi, J. K. (1993) *Biophys. J.* **65,** 124–130.
8. Moltke, S., Krebs, M. P., Mollaaghababa, R., Khorana, H. G. & Heyn, M. P. (1995) *Biophys. J.*, in press.
9. Tittor, J., Schweiger, U., Oesterhelt, D. & Bamberg, E. (1994) *Biophys. J.* **67,** 1682–1690.
10. Krebs, M. P., Mollaaghababa, R. & Khorana, H. G. (1993) *Proc. Natl. Acad. Sci. USA* **90,** 1987–1991.
11. Otto, H., Marti, T., Holz, M., Mogi, T., Lindau, M., Khorana, H. G. & Heyn, M. P. (1989) *Proc. Natl. Acad. Sci. USA* **86,** 9228–9232.
12. Holz, M., Lindau, M. & Heyn, M. P. (1988) *Biophys. J.* **53,** 623–633.
13. Holz, M., Drachev, L. A., Mogi, T., Otto, H., Kaulen, A. D., Heyn, M. P., Skulachev, V. P. & Khorana, H. G. (1989) *Proc. Natl. Acad. Sci. USA* **86,** 2167–2171.
14. Polster, J. & Lachmann, H. (1989) *Spectrometric Titrations* (VCH, New York).
15. Száraz, S., Oesterhelt, D. & Ormos, P. (1994) *Biophys. J.* **67,** 1706–1712.
16. Kataoka, M., Kamikubo, H., Tokunaga, F., Brown, L. S., Yamazaki, Y., Maeda, A., Sheves, M., Needleman, R. & Lanyi, J. K. (1994) *J. Mol. Biol.* **243,** 621–638.